February 25, 1976

ANL-FRA-TM-85

SODIUM VOIDING CALCULATIONS IN A CRBR MODEL AND COMPARISONS WITH ZPPR EXPERIMENTS

R. W. Schaefer

Applied Physics Division
Argonne National Laboratory
9700 South Cass Avenue
Argonne, Illinois 60439

FRA TECHNICAL MEMORANDUM NO. 85

Results reported in the FRA-TM series of memoranda frequently are preliminary and subject to revision. Consequently they should not be quoted or referenced without the author's permission.

Work performed under the auspices of the U. S. Atomic Energy Commission.

The facilities of Argonne National Laboratory are owned by the United States Government. Under the terms of a contract (W-31-109-Eng-38) between the U. S. Energy Research and Development Administration, Argonne Universities Association and The University of Chicago, the University employs the staff and operates the Laboratory in accordance with policies and programs formulated, approved and reviewed by the Association.

MEMBERS OF ARGONNE UNIVERSITIES ASSOCIATION

The University of Arizona
Carnegie-Mellon University
Case Western Reserve University
The University of Chicago
University of Cincinnati
Illinois Institute of Technology
University of Illinois
Indiana University
Iowa State University
The University of Iowa
Kansas State University
The University of Kansas
Loyola University
Marquette University
Michigan State University
The University of Michigan
University of Minnesota
University of Missouri
Northwestern University
University of Notre Dame
The Ohio State University
Ohio University
The Pennsylvania State University
Purdue University
Saint Louis University
Southern Illinois University
The University of Texas at Austin
Washington University
Wayne State University
The University of Wisconsin

Sodium Voiding Calculations in a CRBR Model and Comparisons with ZPPR Experiments

R. W. Schaefer

Applied Physics Division
Argonne National Laboratory
Argonne, Illinois 60439

FRA TECHNICAL MEMORANDUM NO. 85

Work performed under the auspices of the U. S. Energy Research and Development Administration.

Sodium Voiding Calculations in a CRBR Model and Comparisons with ZPPR Experiments

R. W. Schaefer

Applied Physics Division
Argonne National Laboratory
Argonne, Illinois 60439

ABSTRACT

The effect of certain parameters on the calculated sodium void worth in a CRBR model is investigated. The fuel composition and the control rods strongly influence the void worth. The version of delayed data has a less strong but still significant impact. With 27 group results as a standard, the void worth obtained using 21 groups is an unexpectedly small improvement over the nine group worth.

Comparisons between sodium voiding calculations on the CRBR model and selected ZPPR voiding results are made. When the factors above are accounted for, the CRBR calculations are in satisfactory agreement with ZPPR calculations.

TABLE OF CONTENTS

LIST OF TABLES

LIST OF FIGURES

I. INTRODUCTION

A preliminary calculation of reactivity for extensive sodium voiding in a Clinch River Breeder Reactor (CRBR) model appeared to be markedly higher than voiding worths in ZPPR assemblies. The apparent discrepancy prompted this study of factors affecting the calculated void worth in the CRBR model and comparisons with ZPPR voiding results.

Background information is presented first and this is followed by the results. In Section II we describe the calculational method, the reactor model and cross sections used in the study. In Section III the effects of several factors on sodium void worth are described. The factors examined are delayed data and number of broad groups, the presence of control rods and other regions, and the fuel type. Comparisons with selected ZPPR results are made in Section III.5. A summary of results and conclusions comprise the final section.

II. BACKGROUND

II.1. Method

Void worths were calculated using the two-dimensional diffusion theory quasistatic kinetics code FX2[1,2]. The void worths were obtained by voiding, in a step fashion, a zone of the reactor model. The resulting transient was followed for a single time step 10 msec. in length. The reactivity, ρ, effective delayed neutron fraction, β_{eff}, and the other kinetics parameters are evaluated at the end of the time step according to their integral definitions.

The one-step quasistatic reactivity is similar to a static, adiabatic reactivity ($\rho = \frac{k-k_o}{k}$). The quasistatic and adiabatic flux calculations differ in two ways: 1) the quasistatic equation contains the time derivative term, $\frac{1}{v}\frac{\partial\phi}{\partial t}$ not present in the static equation, and 2) the quasistatic equation has a time-varying pointwise precursor source whereas the adiabatic equation has the asymptotic precursor source. The methods have been found to yield reactivities which agree to within 1%, indicating that those differences are not important in the CRBR void calculations.

II.2. Reactor Model

The calculations were performed using an R-Z model of the CRBR. Figure 1 shows the base case model including region labels and dimensions, and the spatial mesh. The base case contains a two zone core, blankets, surrounding regions on all sides and control rods which are partially inserted in the center and on the flats of the hexagonal ring seven. The mesh spacing is non uniform but generally is 5-6 cm.

Beginning of first cycle material compositions were used. Most of the calculations used LWR-grade mixed oxide fuel but some cases did use FFTF-grade fuel. The plutonium isotopic ratios for these two fuel types are shown in Table I. The isotopic composition of each region may be obtained from data presented in Appendix A.

II.3. Cross Sections

The broad group cross section sets used in the calculations are based on ENDF/B Version-III data. The sets were generated with material compositions corresponding to an unvoided, beginning of first cycle CRBR model fueled with LWR-grade mixed oxide fuel.

A single 212 group cross section set, which excluded fission and capture resonances, was generated using MC^2-2[3]. Then each broad group set was produced from the 212-group set using the SDX code[4]. The inner core, outer core and blanket were treated heterogeneously while a homogeneous treatment was used for the reflector region. A four region one-dimensional diffusion theory calculation collapsed the data to a broad group set.

The lethargy widths for the various broad group sets are shown in Table II.

Most of the sets have all cross sections at 1100°K. Two, however, contain cross sections at four different temperatures. For these two sets, FX2 uses a four point interpolation scheme to obtain fission and capture cross sections at the user-specified temperature of each region.

The two forms of delayed data used in most of the calculations have two undesirable properties. The more serious problem is that the delayed family 1 emission spectrum is used for all families. A minor weakness is the use of decay constants inconsistent with the precursor yield data; default values from the ARC System module CSI007 were used (see page 587 of

One of the versions, KBH.DLAY, contains the Batchelor and Hyder (^{235}U) delayed family 1 emission spectrum. Keepin fast fission yield data are used. The second version, F1V4.DLAY, contains the ENDF/B-Version-IV ^{238}U delayed family 1 emission spectrum. The yield data are from ENDF/B-Version-IV.

A corrected delayed data set, V4.DLAY, was created recently and was used in a few cases. This data set has family-dependent ^{239}Pu delayed emission spectra from ENDF/B-Version-IV. Version-IV yield data are also used. The decay constants are the average decay constants for LWR-grade fuel appearing in Table 4.3-33 of Ref. 5.

III. RESULTS

III.1. Effect of Cross Sections

Many of the calculations in this study used nine group cross section sets. In contrast, ZPPR calculations typically use about three times as many groups. In addition, the delayed data in this study are different from data used in ZPPR analyses.

Sensitivity of the void worth to the number of broad groups and to the delayed data is shown in Table III. For all of these calculations the following conditions applied: 1) LWR-grade fuel was used, 2) all cross sections were at 1100^{o}K and 3) the regions voided were the entire core and regions above. The percent error entries are errors relative to the ANL 27 group results using the same delayed data.

Comparison of results using the two nine group sets shows essentially the same values for all quantities of interest. The two structures differ only in the lethargy widths of groups eight and nine.

It can be seen from Table III that, as the number of group increases, the initial k_{eff} increases while ρ/β decreases. In steady-state calculations, the nine group values of k_{eff} differ from the 27 group values by approximately 0.15%. The 21 group value has an error one third as large. In the transient calculations the 21 group results are a surprisingly small improvement over the nine group values.

The form of delayed data had a negligible impact on k_{eff}. In contrast, the delayed data did affect reactivity measured in dollars. Between results using KBH.DLAY and F1V4.DLAY, β_{eff} increased by 9-13% leading to reactivity values which are 15-20¢ smaller. Using the corrected Version-IV form, V4.DLAY, increased β_{eff} 3% over the value using F1V4.DLAY, thus lowering the reactivity by a few cents. The final case, using the same Keepin and Batchelor and Hyder data as KBH.DLAY except with a family-dependent

delayed spectrum, had a void worth 5¢ lower than the corresponding case using KBH.DLAY. These last two results are fortunate since they indicate that the incorrect delayed spectra did not have serious consequences.

III.2. Effect of Regions Present

Differences in geometry and structure between the CRBR model and ZPPR assemblies are numerous. The pin vs plate structure has been explored in ZPPR experiments. In this section we examine the effect of control rods and the lower most regions. The base case CRBR model has partially inserted control rods. In contrast some ZPPR assemblies have no control rods, others have control positions but no B_4C and still others have parked control rods. Dimensions and compositions of the upper-most and lower-most regions differ among ZPPR assemblies and all of these differ from the CRBR model.

The base case model has central and ring seven flats control rods inserted 62 cm. into the core. The parked rods configuration has all rods in the upper blanket and plenum with rod tips at the core-blanket interface. All the control rings below the tips are the same as ring four in the base case. In the no control rods cases, the rods and control channels are replaced by the composition of the surrounding region.

For all calculations in this section, the following conditions applied: 1) the regions voided were the lower blanket, the entire core and regions above, 2) the WARD nine group cross section structure and KBH.DLAY data set were used, 3) a time-independent, regionwise-averaged full power temperature distribution was imposed and 4) the base case spatial mesh was used.

The results are shown in Table IV. The sensitivity of the void worth to the control rods is striking. The worth with parked rods is less than the worth with partially inserted control rods by more than a factor of two. It is conjectured that differences in the flux gradient are the

primary source of this effect; in Appendix B heuristic explanations of the control rod effect are given.

The effect of the lower regions is seen by comparing the last two cases. Removing the rod attachment region and the lower shield reduces the void worth by 23¢. This also may be attributed to the change in the flux gradient.

III.3. Effect of Fuel Type

Most of the calculations in this study used the LWR-grade mixed oxide fuel composition originally proposed for the CRBR first core. The ZPPR assemblies use FFTF-grade fuel and the difference in the plutonium isotopic mix can affect sodium void worth. Accordingly, several cases were run using FFTF-grade fuel for comparison.

Table V shows the effect of fuel type for different situations, 1) nine groups vs 27 groups and 2) voiding the entire core plus regions above vs voiding the inner core plus regions above. In all cases the void worth is approximately 50¢ higher with FFTF-grade fuel.

These results are in general agreement with data in Section 4.3.5 of the PSAR, Ref. 5. The PSAR values of void worth are roughly 70¢ higher for FFTF-grade fuel.

The six fold smaller ^{241}Pu content in the FFTF-grade fuel (replaced by ^{239}Pu) is the primary cause of the void worth increase. Trading ^{239}Pu for ^{241}Pu is known to strongly increase the (positive) spectral component of the void worth[11]. The change in ^{240}Pu content from 19% to 12% is substantial but this change is not the important factor. Measurements in ZPR-6 assembly 7 showed little effect on central void worth from high ^{240}Pu content[6]. Measurements in ZPPR-4 show an increased void worth in the high ^{240}Pu sector but the primary cause there may have been changes in the flux gradient rather than spectral effects[7]. At a constant fertile-to-fissile

ratio, an increase in the (positive) spectral component of void worth with increasing ^{240}Pu content is expected[11].

III.4. Void Worth vs. Zone Voided

Data on the worth of voids in different regions of the CRBR model are useful in comparisons with ZPPR experiments. Void worths computed for four different void zones are presented in Table VI. All calculations for this table used LWR-grade fuel, the base case model and nine group cross sections.

Assuming the void worth for a region to be independent of the sodium concentration in neighboring regions can be a good approximation. For example, voiding the lower blanket alone, case three, yields a reactivity of -42¢ whereas the worth found by taking the difference between cases one and two is -43¢. On this basis, cases four and five imply that the void worth for the outer core plus regions above is -97¢.

III.5. Specific Comparisons with ZPPR Results

Two cases have been run which attempt to simulate voiding cases reported for ZPPR's. An extensive voiding case is also compared.

The first calculation approximates the ZPPR-2 93 drawer voiding experiment. The model used FFTF-grade fuel and did not contain control rods or rod positions. The voided central zone, shown in Fig. 2, is similar to the 93 drawer zone. The void worth calculated using 27 group cross sections at $1100^{o}K$ was 90¢ or $\rho = 2.85 \times 10^{-3}$. This is 32% higher than the calculated worth for ZPPR-2, 218 inhours or $\rho = 2.16 \times 10^{-3}$[8]. The causes of this difference are discussed below.

The second calculation is for a configuration similar to ZPPR-5 Phase A. The model had all control rods parked in the upper axial blanket and used FFTF-grade fuel. The zone voided is the inner core between the central control rod channel and the ring four control rod channels. Except

for some voiding in the ZPPR within ring four, this zone is similar to ZPPR-5 zones 1B+1C+1D. The calculation employed 27 group cross sections at 1100°K and used V4.DLAY delayed data. Table VII shows that the reactivity for this case is 89¢. This is 16¢ or 22% higher than the reactivity reported in Table XI of Ref. 8. The ZPPR-5 calculations were performed using 28 group cross sections from ENDF/B-Version IV data.

A very approximate comparison for extensive voiding can be made from data already presented. Summing the worths for all the void zones in Table XI of Ref. 9 results in an extensive void in ZPPR-5 Phase A worth $1.43. A worth for the CRBR may be obtained as follows: starting with the parked rods case in Table IV (56¢), add 42¢ for the lower blanket not being voided (Table VI). Then, according to Table III, approximately 30¢ is subtracted in going from nine group temperature-dependent cross sections with KBH.DLAY to 27 group 1100°K cross sections with F1V4.DLAY. Finally add 50¢ for FFTF fuel (Table V), resulting in an extensive void worth ~$1.20.

These two numbers should not be compared directly for at least two reasons. The ZPPR-5 void did not include half of the outer core and blanket above and also left unvoided a small ring in the inner core and blanket above near ring seven. This is probably a net negative void effect which is present in the CRBR case.

Secondly, the ZPPR-5 analysis was done using Version-IV cross sections and delayed data and used sodium-out cross sections in voided regions. The CRBR calculations used Version-III cross sections, only sodium-in values, and used F1V4.DLAY. Reference 9 indicates void worths approximately 25% higher with Version-IV data but some of this is due to changes in delayed data and changes in the SDX processing code.

With these factors in mind, it appears that the CRBR and ZPPR extensive void worths are consistent.

IV. SUMMARY

A number of factors which significantly affect sodium void worths have been examined. Accounting for these factors is important when comparing the CRBR calculations with ZPPR results. Specific comparisons with ZPPR calculations have been assessed.

The delayed data, through their effect on β_{eff}, have an impact on void worth. In going from KBH.DLAY to V4.DLAY the worth of an extensive void decreases by almost 20¢ or 13%.

Extensive voiding worths calculated with 27 group cross sections are lower than results obtained with nine group cross sections by 10-15%. Using 27 group results as a standard, there is a surprisingly small improvement in computed reactivity obtained with 21 groups instead of nine. This suggests the possibility that 27 groups may not be sufficient, that using more groups may change the void worth. Alternatively, there may be some problem with the cross section sets used in the study. This question should be examined further.

Control rods have been found to strongly affect the void worth. In the parked rods configuration, the extensive voiding worth is much lower (> 50%) than in either the rods partially in or no rods configurations. This indicates that it is very important in making comparisons with ZPPR results to match the control rod configurations.

The effect of fuel type on sodium void worth also is pronounced. ZPPR assemblies use FFTF-grade mixed oxide fuel whereas, until recently, LWR-grade fuel was proposed for the CRBR first core. When the model contains FFTF-grade fuel, worths for extensive voiding are 50¢ higher than when the LWR mix is used.

Comparisons between CRBR calculations in this study and analogous ZPPR voiding cases show satisfactory agreement. The CRBR results are consistently higher than the corresponding ZPPR cases but the differences are less than 35%.

There are numerous factors which may cause these differences. The ZPPR plate structure vs. the CRBR pin structure is one factor; Table XI of Ref. 9 indicates that void worths are higher in a pin matrix. The temperature difference between the zero power assemblies and the CRBR models is another factor; nine group calculations have shown that changing the CRBR fuel temperature from a full power distribution (inner core 1395^{o}K, outer core 1256^{o}K) to a constant 1100^{o}K reduces the extensive void worth by eight cents. Other factors which may contribute include use of different cross section modeling and data as well as region composition and dimension differences between the CRBR model and the ZPPR assemblies.

REFERENCES

1. T. A. Daly, D. R. Ferguson and R. W. Schaefer, "FX2, A Quasistatic Multidimensional Multigroup Diffusion Theory Code", ANL Topical Report to be published.
2. D. A. Meneley, et al., "A Kinetics Model for Fast-Reactor Analysis in Two-Dimensions", Dynamics of Nuclear Systems, The University of Arizona Press, Tuscon, Arizona (1972), pp 483-500.
3. C. G. Stenberg and A. Lindeman, "The ARC System Cross-section Generation Capabilities, ARC-MC^2", ANL-7722 (1973).
4. H. Henryson, II, et al., "A User's Manual for the Intermediate-Group Spatially Dependent Multigroup Cross-Section Capability, SDX", FRA-TM-33 (1972).
5. "Clinch River Breeder Reactor Project Preliminary Safety Analysis Report", Project Management Corporation.
6. E. M. Bohn, et al., "Measurements in ZPR-6 Assembly 7 with the High-240 Plutonium Zone", ANL-7910, Applied Physics Division Annual Report, July 1970 - June 1971, p. 102.
7. H. F. McFarlane and C. L. Beck, "The High - ^{240}Pu Sector Experiments in ZPPR Assembly 4", ZPR-TM-211 (1975).
8. C. L. Beck and G. L. Grasseschi, "Analysis of Selected ZPPR-2 Sodium Voided Configurations", ZPR-TM-173 (1974).
9. C. L. Beck, et al., "Status of Sodium Voiding Analysis", unpublished.
10. A. F. Henry, Nuclear-Reactor Analysis, M.I.T. Press, Cambridge, Mass. (1975).
11. H. H. Hummel and D. Okrent, Reactivity Coefficients in Large Fast Power Reactors, American Nuclear Society (1970).

TABLE I. Ratio of Plutonium Isotopes in Fuel Types

Pu^i	$Pu^i / \sum_i Pu^i$	
	FFTF-Grade	LWR-Grade
^{238}Pu	-	0.010
^{239}Pu	0.864	0.673
^{240}Pu	0.117	0.192
^{241}Pu	0.017	0.101
^{242}Pu	0.002	0.024

TABLE II. Group Lethargy Widths of Cross Section Sets

Set / Group	WARD9	ANL9	21	ANL27
1	1.5	1.5	0.5	0.5
2	1.0	1.0	0.5	0.5
3	1.5	1.5	0.5	0.5
4	1.5	1.5	0.5	0.5
5	1.5	1.5	0.5	0.5
6	1.5	1.5	0.5	0.5
7	1.5	1.5	0.5	0.5
8	6.5	4.5	0.5	0.5
9	∞	∞	0.5	0.5
10			0.5	0.5
11			0.5	0.5
12			0.5	0.5
13			0.5	0.5
14			0.5	0.5
15			0.5	0.5
16			0.5	0.5
17			0.5	0.5
18			1.0	0.5
19			2.0	0.5
20			3.0	0.5
21			∞	0.5
22				1.0
23				1.0
24				1.0
25				1.0
26				1.0
27				∞

TABLE III. Cross Section Comparison for Extensive Voiding in CRBR

Cross Sections		Steady State Multiplication Factor		Reactivity (Dollars)		$\rho \times 10^3$	$\beta \times 10^3$
Delayed Version	Group Structure	k_{eff}	% Error	ρ/β	% Error		
KBH.DLAY	WARD9G	0.9941	0.15	1.57	9.8	4.99	3.18
KBH.DLAY	21G	0.9950	0.06	1.54	7.7	4.75	3.08
KBH.DLAY	ANL27G	0.9956	-	1.43	-	4.40	3.08
F1V4.DLAY	WARD9G	0.9940	0.14	1.42	14.5	4.99	3.50
F1V4.DLAY	ANL9G	0.9940	0.14	1.42	14.5	4.99	3.50
F1V4.DLAY	21G	0.9949	0.05	1.34	8.1	4.75	3.54
F1V4.DLAY	ANL27G	0.9954	-	1.24	-	4.39	3.54
V4.DLAY	WARD9G	0.9941		1.39		4.99	3.60
NEW.KBH.DLAY	WARD9G	0.9942		1.52		4.99	3.29

TABLE IV. Void Worth vs Regions Present in the CRBR Model

Case	Departure from Base Case Model	Reactivity (Dollars)	Initial k_{eff}
1	Base Case (Central CR. and Ring 7 Flat CR's Partially in Core)	1.22	0.995
2	All Control Rods Parked in Upper Blanket	0.56	1.039
3	No Control Rods Present	1.39	1.090
4	No Control Rods, Shield or Rod Attachment Regions Present	1.16	1.089

TABLE V. Effect of Fuel Type on Void Worth

Fuel Type	Cross Sections	Voided Regions	Reactivity (Dollars)	$\rho \times 10^{-3}$	$\beta \times 10^{-3}$	Initial k_{eff}
LWR	ANL27G, F1V4.DLAY	Core and Regions	1.24	4.39	3.54	0.9954
FFTF	ANL27G, F1V4.DLAY	Above	1.76	5.70	3.24	0.9929
LWR	WARD9G, F1V4.DLAY	Core and Regions	1.42	4.99	3.50	0.9940
FFTF	WARD9G, F1V4.DLAY	Above	1.93	6.17	3.20	0.9914
LWR	WARD9G, F1V4.DLAY	Inner Core and	2.39	8.29	3.47	
FFTF	WARD9G, F1V4.DLAY	Regions Above	2.89	9.15	3.17	

TABLE VI. Voided Zone vs Void Worth

Case	Voided Regions	Cross Sections	Temperature Profile	Reactivity (Dollars)	$\rho \times 10^{-3}$	$\beta \times 10^{-3}$	Initial k_{eff}
1	Lower Blanket + Core + Regions Above	WARD9G, KBH.DLAY	Full Power	1.22	3.89	3.18	0.9948
2	Core + Regions Above	WARD9G, KBH.DLAY	Full Power	1.65			0.9948
3	Lower Blanket	WARD9G, KBH.DLAY	Full Power	-0.42	-1.27	3.07	0.9948
4	Core + Regions Above	WARD9G,F1V4.DLAY	1100°K	1.42	4.99	3.50	0.9940
5	Inner Core + Regions Above	WARD9G, F1V4.DLAY	1100°K	2.39	8.29	3.47	0.9940

TABLE VII. Specific Comparisons with ZPPR Calculations

Voided Regions	Cross Sections	Reactivity (Dollars)	$\rho \times 10^3$	$\beta \times 10^3$	Initial k_{eff}
ZPPR-2 "93 Drawer" Zone	27G, F1V4.DLAY	0.901	2.85	3.16	1.087
ZPPR Calculations	27G ENDF/B V3		2.16[1]		
ZPPR5 Zones "1B + 1C + 1D"	27G, V4.DLAY	0.890	2.91	3.27	1.0375
ZPPR Calculations	28G, V4	0.733[2]			

[1]Reference 8 Table VIII

[2]Reference 9 Table XI

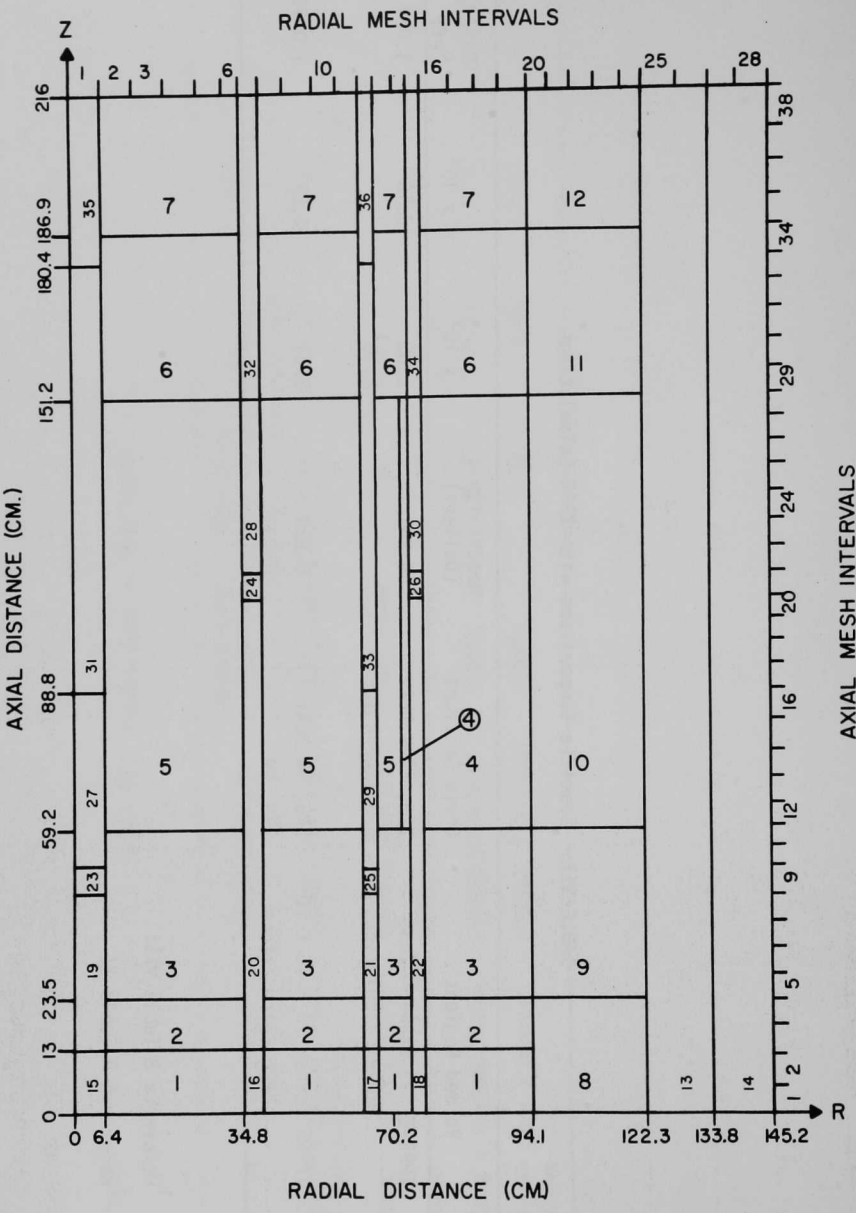

Fig. 1. Base Case CRBR Model

Region Number	Region Label	Comments
1	SHIELD	Lower shield
2	RODATT	Rod attachment
3	LAXBKT	Lower axial blanket
4	OUCORE	Outer core
5	INCORE	Inner core
6	UAXBKT	Upper axial blanket
7	FGPLEN	Fission gas plenum
8	RATBKT	Rod attachment
9	LAEBKT	Radial blanket-lower extension
10	RDLBKT	Radial blanket
11	UAEBKT	Radial blanket-upper extension
12	FGPBKT	Fission gas plenum
13	RDLREF	Radial reflector
14	RDLRST	Radial restraint
		Control rod regions; first 3 label characters specify function and last 3 specify rod ring
15-18	SHDCR1-SHDCR4	Shield
19-22	SODCR1-SODCR4	Sodium-filled channel
23-26	RATCR1-RATCR4	Rod attachment
27-30	LPLCR1-LPLCR4	Lower plenum
31-34	B4CCR1-B4CCR4	Boron control rods
35,36	UPLCR1,UPLCR3	Upper plenum
		CR1 = central control rod channel CR2 = hex. ring 4 control rod channel CR3 = flats of hex. ring 7 control rod channel CR4 = corners of hex. ring 7 control rod channels

Fig. 1. Base Case CRBR Model (Contd.)

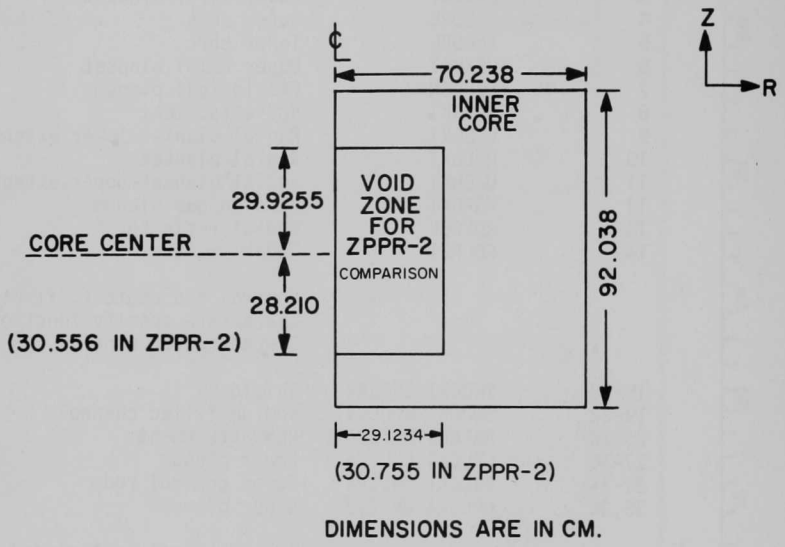

Fig. 2. Voided Zone in CRBR Model for ZPPR-3 93 Drawer Comparison

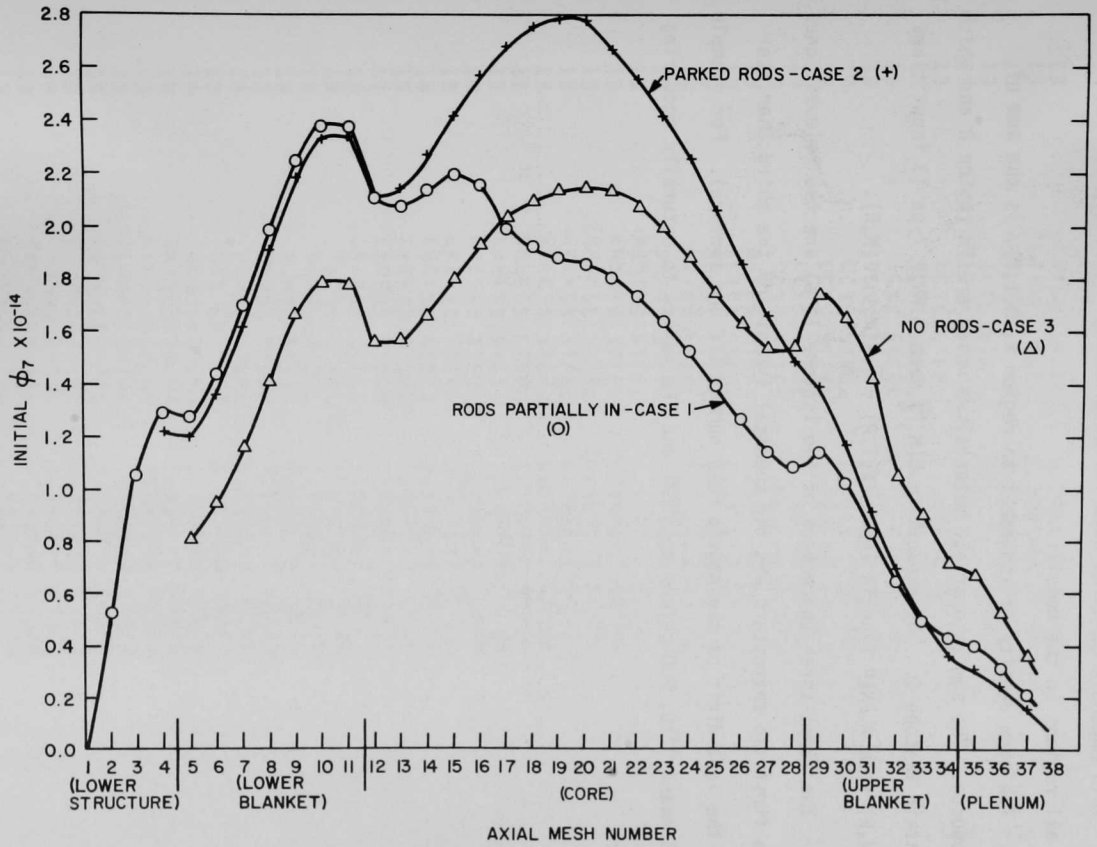

Fig. 3. Initial Group 7 Flux in Radial Mesh Interval 2 vs. Axial Mesh Number (WARD9G Cross Section Structure)

APPENDIX A

This Appendix contains data for determining the isotopic composition of all regions in the model.

The atom density of isotope I in region R, N(I,R), is the sum of products. The sum is over all materials M which are in region R and which contain isotope I. The product is N(M,I) from A.FNIP Type 13 input times F(M,R) from A.FNIP Type 14 input; $N(I,R) = \sum_{M} N(M,I)*F(M,R)$.

The first three characters of the isotope label are the relevent ones. The first two characters are the chemical symbol and the third character is the last digit of the atomic mass number (if one isotope). For example, U-5 means ^{235}U, PUO refers to ^{240}Pu and FEN refers to naturally occurring Fe.

APPENDIX A.

A.FNIP TYPE 13 CARD INPUT

	M		N(M,I)	I
13	BKTFUL	FUEL	5.075E-5	U-5AB
13	BKTFUL	FUEL	2.302E-2	U-8AB
13	BKTFUL	FUEL	4.614E-2	O-6AB
13	ICSS	STEEL	5.480E-2	FENAI
13	ICSS	STEEL	1.591E-2	CRNAI
13	ICSS	STEEL	1.087E-2	NINAI
13	ICSS	STEEL	1.232E-3	MONAI
13	ICSS	STEEL	1.505E-3	MN5AI
13	UCSS	STEEL	5.480E-2	FENAU
13	UCSS	STEEL	1.591E-2	CRNAU
13	UCSS	STEEL	1.087E-2	NINAU
13	UCSS	STEEL	1.232E-3	MONAU
13	UCSS	STEEL	1.505E-3	MN5AU
13	BKTSS	STEEL	5.480E-2	FENAB
13	BKTSS	STEEL	1.591E-2	CRNAB
13	BKTSS	STEEL	1.087E-2	NINAB
13	BKTSS	STEEL	1.232E-3	MONAB
13	BKTSS	STEEL	1.505E-3	MN5AB
13	RRSTSS	STEEL	6.138E-3	FENAR
13	RRSTSS	STEEL	1.459E-2	CRNAR
13	RRSTSS	STEEL	6.463E-2	NINAR
13	RREFSS	STEEL	4.761E-2	FENAR
13	RREFSS	STEEL	1.578E-2	CRNAR
13	RREFSS	STEEL	1.914E-2	NINAR
13	RREFSS	STEEL	1.049E-3	MONAR
13	RREFSS	STEEL	1.283E-3	MN5AR
13	LREFSS	STEEL	5.509E-2	FENAR
13	LREFSS	STEEL	1.599E-2	CRNAR
13	LREFSS	STEEL	1.093E-3	NINAR
13	LREFSS	STEEL	1.238E-3	MONAR
13	LREFSS	STEEL	1.514E-2	MN5AR
13	PLMSS	STEEL	5.499E-2	FENAR
13	PLMSS	STEEL	1.596E-2	CRNAR
13	PLMSS	STEEL	1.058E-2	NINAR
13	PLMSS	STEEL	1.146E-3	MONAR
13	PLMSS	STEEL	1.516E-3	MN5AR
13	ICSODCOOLNT		2.205E-2	NA3AI
13	UCSODCOOLNT		2.207E-2	NA3AU
13	BKTSODCOOLNT		2.226E-2	NA3AB
13	REFSODCOOLNT		2.254E-2	NA3AR
13	ICNB4CCONTRL		1.961E-2	B-0AI
13	ICNB4CCONTRL		7.952E-2	B-1AI
13	ICNB4CCONTRL		2.591E-2	C-2AI
13	BKNB4CCONTRL		1.961E-2	B-0AB
13	BKNB4CCONTRL		7.952E-2	B-1AB
13	BKNB4CCONTRL		2.591E-2	C-2AB
13	BKEB4CCONTRL		3.963E-2	B-0AB
13	BKEB4CCONTRL		5.962E-2	B-1AB
13	BKEB4CCONTRL		2.593E-2	C-2AB

A.FNIP TYPE 13 CARD INPUT

	M		N(M,I)	I

IF LWR-GRADE FUEL

13	ICFUL	FUEL	3.971E-5	PU8A1
13	ICFUL	FUEL	2.672E-3	PU9A1
13	ICFUL	FUEL	7.623E-4	PU0A1
13	ICFUL	FUEL	4.010E-4	PU1A1
13	ICFUL	FUEL	9.531E-5	PU2A1
13	ICFUL	FUEL	1.231E-4	U-5A1
13	ICFUL	FUEL	1.721E-2	U-8A1
13	ICFUL	FUEL	4.176E-2	U-6A1
13	UCFUL	FUEL	5.806E-5	PU8AU
13	UCFUL	FUEL	3.907E-3	PU9AU
13	UCFUL	FUEL	1.115E-3	PU0AU
13	UCFUL	FUEL	5.864E-4	PU1AU
13	UCFUL	FUEL	1.394E-4	PU2AU
13	UCFUL	FUEL	1.114E-4	U-5AU
13	UCFUL	FUEL	1.558E-2	U-8AU
13	UCFUL	FUEL	4.212E-2	U-6AU

IF FFTF-GRADE FUEL

13	ICFUL	FUEL	3.217E-3	PU9A1
13	ICFUL	FUEL	4.356E-4	PU0A1
13	ICFUL	FUEL	6.330E-5	PU1A1
13	ICFUL	FUEL	7.447E-6	PU2A1
13	ICFUL	FUEL	1.243E-4	U-5A1
13	ICFUL	FUEL	1.732E-2	U-8A1
13	ICFUL	FUEL	4.234E-2	U-6A1
13	UCFUL	FUEL	4.714E-3	PU9AU
13	UCFUL	FUEL	6.384E-4	PU0AU
13	UCFUL	FUEL	9.275E-5	PU1AU
13	UCFUL	FUEL	1.091E-5	PU2AU
13	UCFUL	FUEL	1.136E-4	U-5AU
13	UCFUL	FUEL	1.580E-2	U-8AU
13	UCFUL	FUEL	4.274E-2	U-6AU

A.FNIP TYPE 14 CARD INPUT

	R / M	F(M,R), M	F(M,R), M	F(M,R)
14	SHIELDLREFSS	.8316REFSUU	.1684	
14	RUDATTLREFSS	.3518REFSUU	.6482	
14	LAXBKTBKTFUL	.3279 BKTSS	.2348BKTSUU	.4240
14	UUCURE UCFUL	.3312 UCSS	.2344 UCSUU	.4169
14	INCURE ICFUL	.3324 ICSS	.2345 ICSUU	.4167
14	UAXBKTBKTFUL	.3273 BKTSS	.2542BKTSUU	.3821
14	FGPLEN PLMSS	.2846REFSUU	.4152	
14	RATBKTLREFSS	.4081REFSUU	.5919	
14	LAEBKTBKTFUL	.5729 BKTSS	.1586BKTSUU	.2588
14	RULBKTBKTFUL	.5725 BKTSS	.1586BKTSUU	.2546
14	UAEBKTBKTFUL	.5725 BKTSS	.1693BKTSUU	.2397
14	FGPBKT PLMSS	.1908REFSUU	.2534	
14	RULREFRREFSS	.8896REFSUU	.1104	
14	RULRSTRRSTSS	.8935REFSUU	.1065	
14	SHUCR1LREFSS	.7800REFSUU	.2200	
14	SUUCR1 BKTSS	.0944BKTSUU	.9056	
14	RATCR1 BKTSS	.4850BKTSUU	.5150	
14	LPLCR1 ICSS	.3604 ICSUU	.3345	
14	B4CCR1ICNB4C	.3174 ICSS	.3287 ICSUU	.3323
14	UPLCR1LREFSS	.3498REFSUU	.3312ICNB4C	0.0
14	SHUCR2LREFSS	.7800REFSUU	.2200	
14	SUUCR2 ICSS	.0944 ICSUU	.9056	
14	RATCR2 ICSS	.4850 ICSUU	.5150	
14	LPLCR2 ICSS	.3607 ICSUU	.3340	
14	B4CCR2BKEB4C	.3172 BKTSS	.3281BKTSUU	.3335
14	SHUCR3LREFSS	.7800REFSUU	.2200	
14	SUUCR3 BKTSS	.0944BKTSUU	.9056	
14	RATCR3 BKTSS	.4850BKTSUU	.5150	
14	LPLCR3 ICSS	.3604 ICSUU	.3345	
14	B4CCR3ICNB4C	.3173 ICSS	.3287 ICSUU	.3323
14	UPLCR3LREFSS	.3498REFSUU	.3312	
14	SHUCR4LREFSS	.7800REFSUU	.2200	
14	SUUCR4 UCSS	.0944 UCSUU	.9056	
14	RATCR4 UCSS	.4850 UCSUU	.5150	
14	LPLCR4 UCSS	.3607 UCSUU	.3340	
14	B4CCR4BKNB4C	.3171 BKTSS	.3280BKTSUU	.3336

APPENDIX B

The effect of regions present in the model on the sodium void worth may be explained qualitatively on the basis of the different flux gradients in the alternative configurations.

In the perturbation expression for reactivity (see, for example, Eq. 7.6.17 of Ref. 10), the leakage change operator, δD, operates on the gradient of the initial flux shape, $\vec{\nabla}\psi_0$. Thus, for a given δD, the smaller $\vec{\nabla}\psi_0$ is, the smaller will be the (negative) leakage term and the more positive the reactivity will be.

In case 3 of Table IV vs. case 4, the presence of the lower structure makes the flux gradient smaller in the lower blanket and in the lower portion of the core. This makes the leakage component of the reactivity smaller and the net reactivity more positive.

For cases 1, 2 and 3 of Table IV, the initial group 7 flux in radial mesh interval 2 is shown in Fig. 3. The gradient in the core is clearly much larger for case 2 than for the other cases. The gradient is so large because the absence of rods in the core allows a high flux there while the presence of rods in the upper blanket supresses the flux in that region. Thus the leakage component is large in case 2 and the net reactivity is much less positive.

The implication of the gradient differences between cases 1 and 3 (see Fig. 3) is unclear but then the difference in void worth between the two cases is not large. Comparing cases 1 and 3 is complicated by the difference in the voided region. In case 1, the control rod channels are not voided and this affects δD, δA etc. This factor tends to make the reactivity lower for case 1 but the magnitude of the effect is small since the rod channels are small.